

## Screened Offset Plates: A Contact Angle Study

Eliane Rousset, Gérard Baudin,<sup>▲</sup> Patrick Cugnet, and André Viallet

*Laboratoire de Génie des Procédés Papetiers, UMR 5518 CNRS/INPG/CTP, Ecole Française de Papeterie et des Industries Graphiques, Domaine Universitaire, Saint Martin d'Hères Cedex; France*

Many studies about offset printing plate surface energetics have dealt with determinations of the difference between image and non-image areas through contact angle measurements. On another hand, contact angle hysteresis studies have highlighted the influence of surface state and/or heterogeneity. The novel approach of Shanahan and Di Meglio expresses hysteresis as a function of surface defects parameters. In the case of offset printing plates we have considered screen dots as defects, and we have evaluated the corresponding hysteresis energy by the use of some liquids such as pure water, glycerol and a series of fountain solutions. The experimental results turned out to validate this approach and to show the way this energy is linked to the screen geometry and the relative dot area. In parallel with this new approach, we have also shown that the classical Cassie and Baxter model of averaging effects may be applied to liquids on screened areas.

Journal of Imaging Science and Technology 45: 517–522 (2001)

### Introduction: The Offset Process

The offset lithographic process is the most important of the major printing processes: its main characteristic is that the image and non-image areas are situated almost at the same level on the printing form (typically an aluminum plate). The ink is supplied to the plate by three or four rubber rollers and transferred to the final printed stock through another rubber surface, i.e., the blanket, as presented in Fig. 1.

In the case of a classical positive presensitized plate, its image and non-image areas are traditionally obtained by placing a positive photographic film, acting as a mask, over the photopolymer coated surface of the plate and exposing it to UV radiation. After a development process mainly consisting in the dissolution of the exposed resin by an alkaline aqueous solution (yielding a hydrophilic alumina surface generating “non-image areas”), a positive image is left on the plate where the unexposed coating (corresponding to oleophilic “image areas”) remains.<sup>1</sup>

Figure 1 shows that the offset plate is installed in the printing group of a press by mounting it on the “plate cylinder” which maintains it in contact with the other rollers. Schematically, the basic sequence of the process consists in a series of fluid transfers by contact between the various surfaces of the cylinders:

a) application over the whole surface of the plate of a thin film of an aqueous solution (the “fountain solu-

tion”) from one or two rollers belonging to the dampening system; we shall come back to this first step in this text;

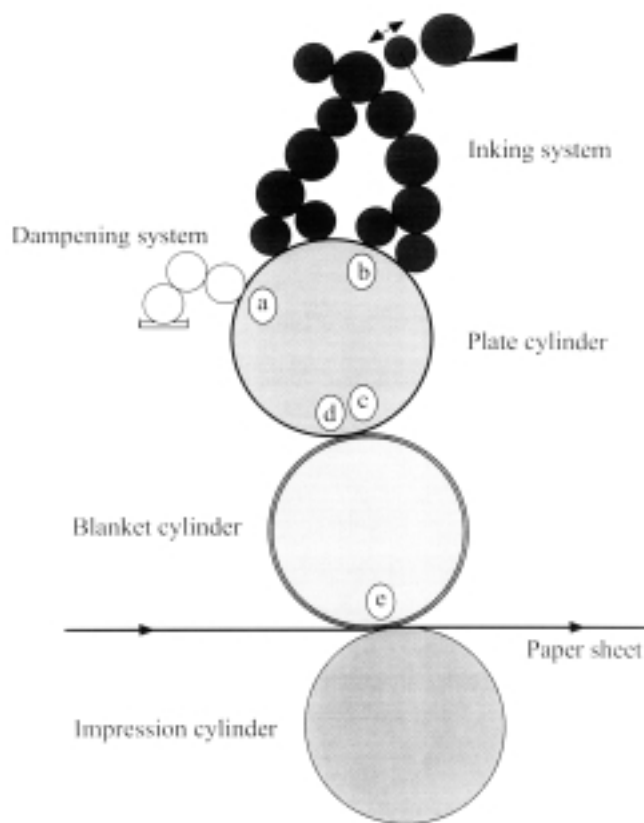


Figure 1..

Original manuscript received March 5, 2001.

▲ IS&T Member

Phone: + 33 (0)4 76 82 69 00; Fax: + 33 (0)4 76 82 69 33;  
E-mail: <gerard.baudin@efpg.inpg.fr>

Previously presented at IS&T's NIP15: International Conference on Digital Printing Technologies, October 17-22, 1999, Orlando, Florida, USA.

©2001, IS&T—The Society for Imaging Science and Technology

- b) application of ink from three or four rollers belonging to the inking system in such a way that the fountain solution is displaced from the image areas and replaced by the ink, while it remains in the non-image areas;
- c) partial transfer of ink from the image areas to the surface of the blanket the compliance of which is designed to enhance the contact with the final printed stock (typically paper);
- d) simultaneously, a proportion of fountain solution is transferred to the blanket directly from the non-image areas of the offset plate and also from the image areas, due to the formation of an emulsion of “water” droplets within the ink phase;
- e) partial transfers of ink and fountain solution from the blanket to the paper.

The above short description obviously shows that the quality of the printed image strongly depends on where the ink and aqueous solution really go. In turn, the transfers are governed by a series of physicochemical parameters among which we shall mention:

- the surface energies of the image and non-image areas on the plate,
- the surface tensions of the ink and fountain solution,
- the dynamic behaviors and balance associated to the distribution of the two liquids, and
- the surface states and energies of the other solid materials involved in the process.

In the case of offset plates, inks and fountain solutions have often been studied in the literature<sup>2,3</sup> separately on image or non image areas. It has been pointed out that the determination of surface energy values was a very helpful way to understand the basics of the fountain solution and ink distribution on these two different areas. On the other hand, to our knowledge, no work was reported about what happens to the fluids when they are brought onto a screened zone consisting of both image- and non-image areas. These surfaces are generated on the plate at a geometric scale around one or two tenths of a millimeter (depending on the value of the screen ruling). This scale is suitable for finding the behaviors of test liquids on heterogeneous surfaces in terms of both hysteretic phenomena and average contact angle evolution on varying technical parameters such as the relative dot area.

This article is a contribution towards a better understanding about the behavior of a continuous film of fountain solution on a screened surface (a feature which corresponds to step (a) of the general offset transfer process). We intended to reach two distinct goals: evaluating to what extent test liquids exhibit a hysteretic phenomenon due to the screened nature of the surface; and confirming the averaging effect of the heterogeneity of offset plate. It is worth keeping in mind some orders of magnitude:

- in the image areas, the photopolymer exhibits a rather low surface energy (35 to 40 mJ/m<sup>2</sup>) that allows a good affinity for inks;
- in the non-image areas, alumina has a strong hydrophilic character, but, for contamination reasons, most of the surface energy measurements yield values ranging from 50 to 85 mJ/m<sup>2</sup>, which are largely lower than that of pure aluminum oxide. Nevertheless, due to its prevalent polar, i.e., non-dispersive, component, this surface promotes the spreading of the aqueous fountain solution.

At this point, let us also remind ourselves of the typical content of a classical fountain solution:

- 87 to 96% water,
- 2 to 10% isopropanol, a liquid which is added to water in order to lower the surface tension of the solution, and is nowadays considered to be unfriendly for human health,
- 2 to 3% concentrated additives (a mixture often of acidic nature).

### Theoretical Background

The basic equation that is always used for the determination of surface energies is the well-known Young's equation:

$$\gamma_{SV} - \gamma_{SL} = \gamma_L \cos\theta \quad (1)$$

where  $\gamma_{SV}$ ,  $\gamma_{SL}$  and  $\gamma_L$  are (provided the thermodynamic equilibrium be obtained) the energies respectively of a flat smooth, solid surface (theoretically saturated by adsorbed molecules from the vapor phase), of the interface between the solid and a liquid, and of the liquid (supposed to be in equilibrium with the vapor). In turn, the solid surface energy is given by:

$$\gamma_{SV} = \gamma_S - \pi_e$$

where  $\gamma_S$  is the energy of the “clean” solid surface and  $\pi_e$  the “spreading pressure” associated with the adsorption of molecules from the vapor phase. A frequent assumption is that this spreading pressure is negligible, an approximation which is fulfilled particularly in the case of “low energy solids” (mainly polymers). In practice, Eq. 1 shows that the higher the contact angle value of a given liquid, the lower the surface energy of the solid. It is important to remember that Young's equation is valid under static conditions (which are not really representative of the offset process). Moreover, Young's equation assumes the existence of only one contact angle value. Actually, when a liquid is laid over a solid, its contact angle may vary between two limits: the upper limit is called the “advancing contact angle”  $\theta_A$  and the lower one the “receding contact angle”  $\theta_R$ ; this phenomenon is known as “contact angle hysteresis”. The fountain solution of the offset printing process exhibits a contact angle hysteresis in the image areas on the plate, but it completely wets the surface of the non-image zones (alumina).

Several decades ago, Wenzel<sup>4</sup> and Cassie and Baxter<sup>5,6</sup> have highlighted the significant influences of surface roughness and heterogeneity on the contact angle values. On the other hand, the basic work of Joanny and de Gennes<sup>7</sup> has lead Shanahan and Di Meglio<sup>8-11</sup> to develop a new approach to the hysteresis phenomenon. Their theoretical considerations yield expressions of the contact angle hysteresis as functions of a set of parameters connected to the surface defects, such as the defect number  $d$  per unit area (defect density) and the equivalent mean radius  $r_d$  of these defects. In the case of a screened offset plate, it is easy to show that these two figures may be calculated from relevant technical parameters (screen ruling  $SR$  and relative screen dot area  $a$ ).

Let us have a further insight into the approach of Shanahan and Di Meglio. The authors present two distinct situations whether the liquid wets or does not wet the “reference surface”, i.e., the surface on which defects are distributed. In fact, the reference surface is wetted when  $\theta = 0$  (or does not exist) and it is not wet-

ted when  $\theta > 0$ . If  $\theta_d$  is the contact angle of the liquid on the surface of the defect itself, the authors also consider the two cases  $\theta > \theta_d$  or  $\theta < \theta_d$ , which mean that the defect may respectively be more wettable or less wettable than the reference surface. This can be quantitatively expressed by a comparison between the work of adhesion of the liquid on the defect ( $W_{ad}$ ) and on the reference substrate ( $W_{ar}$ ). Equation 2, the well-known Dupré's equation, defines any work of adhesion as:

$$W_a = \gamma_S + \gamma_L - \gamma_{SL} \quad (2)$$

By combining Eqs. 1 and 2 and calculating the difference  $\varepsilon = W_{ar} - W_{ad}$ , it is possible to derive Eqs. 3a and 3b:

$$\theta > \theta_d \Rightarrow \varepsilon = \gamma_L(\cos\theta - \cos\theta_d) < 0 \quad (3a)$$

$$\theta < \theta_d \Rightarrow \varepsilon = \gamma_L(\cos\theta - \cos\theta_d) > 0 \quad (3b)$$

The authors' key observation is as follows: if two defects are very close to each other, the effect of one of them on the shape and position of the triple line must be modified by the proximity of the other. They call this effect "shadowing", as if one defect was positioned "in the shadow" of the other. Subsequently, they show that the "shadowing" effect influences the contact angle hysteresis and take this influence into account by applying a correction for the defect density  $d$ . Let  $H$  be the specific energy variation associated to the contact angle hysteresis on a defective surface;  $H$  is defined by Eq. 4:

$$H = \gamma_L (\cos\theta_R - \cos\theta_A) \quad (4)$$

After some complex calculations, found in Refs. 8 through 11, the analysis of Di Meglio and Shanahan yields Eqs. 5a and 5b:

- in the case where the liquid does not wet the reference surface and  $\theta$  is not too large (in practice,  $\theta < 40^\circ$ ):

$$H \sim \frac{\bar{d}L(2r_d\varepsilon)^2}{2\pi\gamma_L\theta^2} \text{ with } L = \ln\left(\frac{r_0}{r_d}\right) + \frac{1}{2}$$

$$\text{and } \bar{d} = d \left[ 1 - \frac{1 + \ln(4r_0^2 d)}{4L} \right] \quad (5a)$$

- in the case where the liquid wets the reference surface:

$$H \sim \frac{\bar{d}(2r_d\varepsilon)^{4/3}}{4(\pi\gamma_L\kappa^2)^{1/3}} \cdot \frac{\ln^{1/2}\left[\coth\left(\frac{\pi}{4\sqrt{2}}r_d\kappa\right)\right]}{\ln^{1/6}\left[\coth\left(\frac{\pi}{2\sqrt{2}}r_d\kappa\right)\right]}$$

$$\text{with } \bar{d} = d - \left[ \frac{8d^{3/2}}{2^{1/3}\pi\kappa\ln^{1/2}\left[\coth\left(\frac{\pi r_d\kappa}{4\sqrt{2}}\right)\right]} \cdot \left[ \exp\left(\frac{-\pi r_d\kappa}{4\sqrt{2}}\right) - \exp\left(\frac{-\pi\kappa}{8\sqrt{2}d^{1/2}}\right) \right] \right] \quad (5b)$$

where the symbols have the following significance:

$\bar{d}$ : corrected defect density (taking "shadowing" into account),

$\kappa^{-1}$ : "capillary length", given by  $(\gamma_L/\rho g)^{1/2}$ ,

$r_0$ : "cut-off distance", a maximum distance at which a defect perturbation on the wetting front (or triple line) may be felt ( $r_0$  has the same order of magnitude as  $\kappa^{-1}$ ),

$\rho$ : density of the liquid,

$g$ : gravitational constant.

It is important to notice that Eqs. 5a and 5b are approximate expressions. As contact angle evolution is a basic feature of the offset process, we have tried to apply the analysis of Shanahan and Di Meglio to this problem. More clearly, we evaluated the hysteresis energy  $H$  associated with the behavior of a fountain solution in the presence of a screened surface on a classical plate. In addition to this first goal, we realized that our experimental data allowed us to calculate advancing and receding contact angle values,  $\theta_{Ac}$  or  $\theta_{Rc}$ . Thus, it became interesting to verify that the Cassie and Baxter approach<sup>5,6</sup> was valid in the cases of advancing or receding contact angles (and not only for the equilibrium angle  $\theta$  of Eq. 1).

$$\cos\theta_{CB} = a \cos\theta_{im} + (1 - a) \cos\theta_{ni} \quad (6)$$

where  $a$  is the relative dot area of the image zone on the screened surface,  $\theta_{im}$  is the contact angle in the image area (photopolymer) and  $\theta_{ni}$  the contact angle in a non-image area (alumina). Finally, these last series of calculations also gave another tool for an evaluation of the hysteresis energy  $H_{CB}$  Eq. 4.

## Experimental

### Methods

The tested substrates were positive anodized grained offset plates; they were processed by the classical method shortly described above (UV irradiation through a screened photographic film and chemical development). The screened areas were characterized by two screen rulings: 40 cm<sup>-1</sup> and 50 cm<sup>-1</sup>, yielding respectively two defect densities  $d = 16 \times 10^6$  m<sup>-2</sup> and  $d = 25 \times 10^6$  m<sup>-2</sup>. The relative dot area  $a$  was varied in both cases from 0 (aluminum oxide surface, non-image zones on the plate) to 1 (photopolymer surface, image zones). The dot area values were determined by an image analysis method. The test liquids were pure water and glycerol (which did not wet either of the two surfaces) on the one hand, and fountain solutions obtained by several dilutions of an offset concentrate into water (which wetted the non-image surface) on the other hand. The proportion of concentrate ranged from 2% to 5%. The surface tensions of these solutions were measured by the Du Noüy ring method (with a Krüss tensiometer).

The contact angle determinations were done by two different techniques:

- by means of the device used in Ref. 3: a video camera to register the shape of a millimeter scale drop, the direct measurements of both the height  $h$  and the contact radius  $r$  of the drop on the captured image, and the derivation of the contact angle by Eq. 7:

$$\tan \frac{\theta}{2} = \frac{h}{r} \quad (7)$$

- by the use of a novel apparatus described in Ref. 12 which allows the measurement of the height of a huge heavy drop (forming a centimeter scale "pancake" on the solid surface) and the derivation of the contact angle by Eq. 8:

TABLE I. Advancing Contact Angle Values

| Liquid        | Screen ruling (cm <sup>-1</sup> ) | Relative dot areas |      |      |      |      |      |      |      |      |      |      |
|---------------|-----------------------------------|--------------------|------|------|------|------|------|------|------|------|------|------|
|               |                                   | 0                  | 0.1  | 0.2  | 0.3  | 0.4  | 0.5  | 0.6  | 0.7  | 0.8  | 0.9  | 1    |
| Water         | 40                                | 22.7               | 36.6 | 41.7 | 44.5 | 51.0 | 59.2 | 73.7 | 76.8 | 78.6 | 83.0 | 89.3 |
| Water         | 50                                | 22.7               | 31.9 | 46.4 | 53.1 | 57.1 | 60.0 | 64.3 | 69.5 | 78.2 | 81.0 | 84.7 |
| Glycerol      | 40                                | 17.3               | 35.4 | 43.2 | 48.6 | 55.2 | 66.6 | 72.1 | 74.7 | 74.8 | 78.7 | 81.0 |
| Glycerol      | 50                                | 24.5               | 30.3 | 45.6 | 47.1 | 56.6 | 61.8 | 65.3 | 70.5 | 74.2 | 74.8 | 81.0 |
| Fount. sol 2% | 40                                | 0                  | 15.5 | 18.3 | 21.5 | 25.9 | 37.9 | 40.4 | 40.6 | 43.5 | 46.8 | 50.5 |
| Fount. sol 2% | 50                                | 0                  | 17.5 | 31.5 | 31.7 | 37.0 | 38.7 | 43.6 | 49.6 | 51.1 | 51.3 | 56.9 |
| Fount. sol 3% | 50                                | 0                  | 13.4 | 18.2 | 25.8 | 28.2 | 30.0 | 34.0 | 35.5 | 39.5 | 41.8 | 50.7 |
| Fount. sol 5% | 50                                | 0                  | 8.2  | 17.0 | 23.1 | 23.6 | 28.1 | 31.3 | 34.1 | 34.6 | 36.1 | 39.2 |

$$\sin \frac{\theta}{2} = \frac{h}{2\kappa^{-1}} \quad (8)$$

The two methods turned out to give quite similar results, which is a strong argument in favor of their reliability.

### Measurements

For contact angle determinations, we principally used the liquid pancake technique: both  $\theta_A$  and  $\theta_R$  were obtained according to Eq. 8. Table I shows typical results corresponding to advancing angles.

The calculations were completed using the following surface tension values:

- Water 72.6 mJ/m<sup>2</sup>
- Glycerol 63.0 mJ/m<sup>2</sup>
- Fountain sol 2% 34.0 mJ/m<sup>2</sup>
- Fountain sol 3% 31.9 mJ/m<sup>2</sup>
- Fountain sol 5% 30.4 mJ/m<sup>2</sup>

The two first values were found in the literature,<sup>2</sup> and the three others were obtained by experiment, as already explained.

### Results: The Approach of Shanahan and Di Meglio

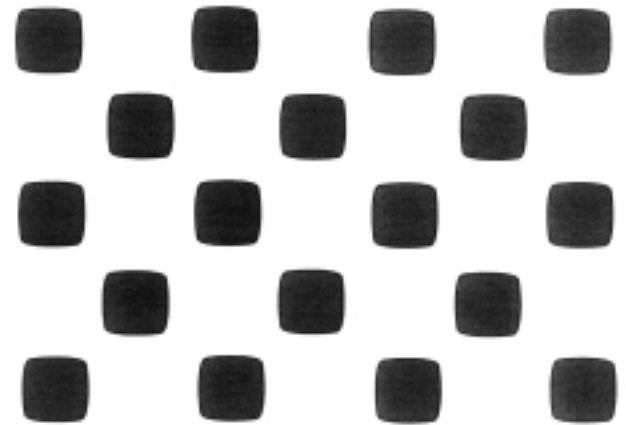
#### Presentation of the Results

From the geometrical point of view, a screened area on an offset plate consists in a regular lattice generally defined by a square element containing an image zone defined by a screen dot (Fig. 2). For a given screen ruling SR, as the relative dot area  $a$  is enhanced, the dimension of a dot grows, and two situations may occur:

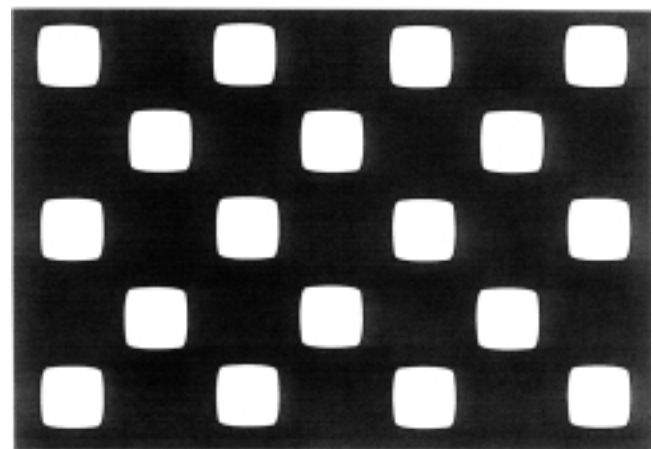
- a) A given dot remains separated from its neighbors: then, it is possible to go over the non-image area continuously, i.e., without being obliged to cross any image zone (Fig. 2, case a). In our case, this situation occurs for  $a \leq 0.6$  and it is reasonable to choose the non-image area as the reference surface according to the definition of Shanahan and Di Meglio; theoretically, this choice corresponds to Eq. 3b, and the printing dots play the role of defects;
- b) On the another hand, a given dot may be connected to its neighbors: then, it is impossible to go over the non-image area continuously (Fig. 2, case b). This situation occurs when  $a > 0.6$  and it would apparently be convenient for the image area be the reference surface in this case.

Nevertheless, we systematically considered the reference surface as that of alumina (non-image area) for two reasons:

- Our experiments show that the hysteresis phenomenon actually occurs in solid image areas, a feature



a: Separated image areas (dots)



b: Separated non-image areas

Figure 2.

which is not explicitly considered for the reference surface in the theoretical developments of Shanahan<sup>8</sup>;

- In order to be valid, Eq. 5a requires that  $\theta$  be not too large, a condition which is almost never fulfilled by our experimental determinations of the contact angles in image areas.

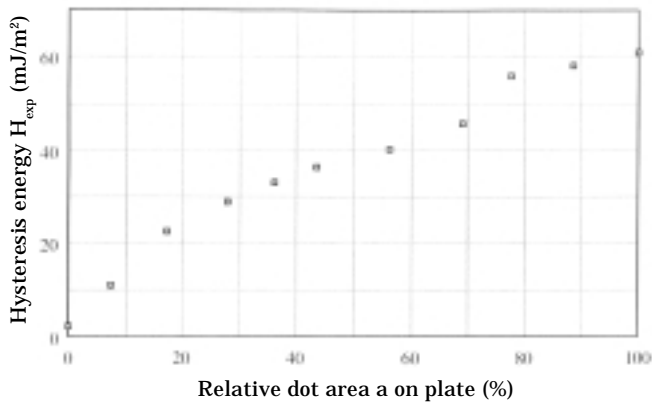


Figure 3.

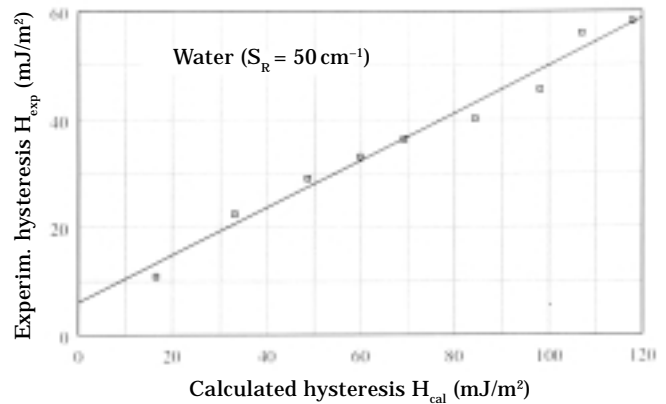


Figure 4.

For further calculations, we used the expressions (5a) for water and glycerol (which did not wet the reference surface) and (5b) for the fountain solutions (which wetted the reference surface). Thus, we obtained calculated values of the hysteresis energy  $H_{cal}$ . Moreover, we also calculated so-called “experimental hysteresis energy”  $H_{exp}$  values by Eq. 4, where  $\theta_A$  and  $\theta_R$  were obtained by measurement. It became possible to plot the variations of  $H_{cal}$  and  $H_{exp}$  as functions of the relative dot area  $a$  for each liquid and each screen ruling. Figure 3 presents a typical result in the case of water with a screen ruling  $SR = 50 \text{ cm}^{-1}$ . Our results globally show that the agreement between the two values of  $H$  is rather moderate, especially in the cases of water and glycerol, where the reference surface was not wetted by the test liquid. Nevertheless, Fig. 4 shows that a linear correlation between  $H_{cal}$  and  $H_{exp}$  does exist. At this point, it is worth adding that a linear correlation was observed for all the tested configurations. Table II gathers the values of the slopes of the straight lines resulting from the same plots as in Fig. 4. An amazing feature to notice from Fig. 4 is that the linear correlation between  $H_{cal}$  and  $H_{exp}$  remains valid even if the value of  $a$  (relative coverage by image areas) is higher than 0.6, a configuration where:

- the surface occupied by defects is larger than the reference surface (non-image area);
- the reference surface becomes discontinuous (as already explained).

Table II shows that the slope values are relatively different from unity, a result which is more easy to see in the cases where the reference surface is not wetted by the liquid (water and glycerol). On the other hand, the screen ruling does not seem to have any evident effect but this fact remains to be verified with other experiments. Although the two tested values ( $40 \text{ cm}^{-1}$  and  $50 \text{ cm}^{-1}$ ) do not vary enough, the choices were due to their frequent utilization in the printing industry. It is also interesting to notice that the “shadowing effect” is important in the case where the liquid does not wet the reference surface (water and glycerol). For example when  $SR = 50 \text{ cm}^{-1}$ , the value of the defect density is lowered down from  $25 \times 10^6$  to  $15.5 \times 10^6$  for  $a = 0.1$  and to  $13 \times 10^6$  for  $a = 0.6$ ; this effect is not so marked when the liquid wets the reference surface (fountain solutions).

## Discussion

Again, it is important to remember that the formulae of Shanahan and Di Meglio, Eqs. 5a and 5b, were derived

TABLE II. Slopes and Correlations Coefficients

| Liquid        | Screen ruling ( $\text{cm}^{-1}$ ) | Slope | Correlation coef. |
|---------------|------------------------------------|-------|-------------------|
| Water         | 40                                 | 0.55  | 0.95              |
| Water         | 50                                 | 0.44  | 0.98              |
| Glycerol      | 40                                 | 0.43  | 0.96              |
| Glycerol      | 50                                 | 0.73  | 0.98              |
| Fount. sol 2% | 40                                 | 1.02  | 0.89              |
| Fount. sol 2% | 50                                 | 0.83  | 0.96              |
| Fount. sol 3% | 50                                 | 0.69  | 0.96              |
| Fount. sol 5% | 50                                 | 1.08  | 0.94              |

with approximations: this is a first reason why the calculated slopes may differ from unity in any experimental configuration. In the cases of water and glycerol, the observed value  $H_{exp}$  (from Eq. 4) on the reference surface (alumina) differs from 0; this is a reason for a lowered value of the calculated slope (cf. Fig. 4); actually, the corresponding estimates of Table I do not exceed 0.73. It is also worth adding that these four configurations are theoretically treated according to Eq. 5a, where the contact angle  $\theta$  of the liquid on the reference surface is explicitly present as its square, i.e., a power index value of 2. Thus, as the measurements yield values around  $20^\circ$ , an absolute uncertainty of  $\pm 4^\circ$  (which is likely to be expected in this range) lead to a relative uncertainty of around 50% in the calculated hysteresis energy  $H_{cal}$ . We think that this is a second reason why the calculated slopes may significantly differ from unity. Moreover, it has already been mentioned that alumina is highly subject to contamination, so that “real” contact angle values are rather difficult to obtain with sufficient reliability, this also has an obvious influence on the results.

In the cases where the reference surface is wetted by the liquid (the fountain solutions fulfill this requirement), no experimental hysteresis occurs on this surface, a feature which is in agreement with the analysis of Shanahan.<sup>8</sup> In addition, these configurations are to be studied according to Eq. 5b, where the contact angle  $\theta$  of the liquid on the reference surface (which is set to 0) no longer appears. Thus, considering the approximate nature of Eq. 5b, it is to be expected that the fountain solutions exhibit  $H_{cal}$  values in fair agreement with the measurements (as may be seen in Table I). On the other hand, the linear behavior of the hysteresis energy  $H$ , for relative dot areas larger than 0.6, seems more diffi-

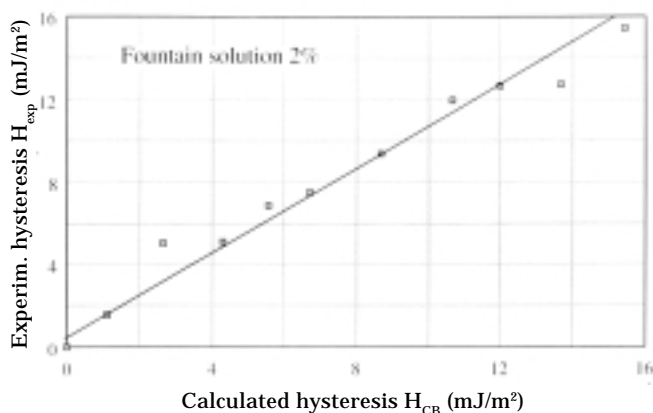


Figure 5.

cult to explain at the present state of our studies. We are led to admit that no evident physical discontinuity governs the wetting of a screened printing surface by a liquid.

### Results: The Approach of Cassie and Baxter

As explained above, it is possible to use our experiments in a second manner. We are led to derive advancing and receding contact angle values on screened surfaces according to Eq. 6, which may be found in Refs. 5 and 6. The calculations are simpler than those corresponding to Shanahan's approach, and they yield another possibility to compare a calculated hysteresis energy,  $H_{CB}$ , with the so-called  $H_{exp}$  (both of them given by Eq. 4). Figure 5 presents a typical result in the case of the fountain solution containing 2% of additive. It may be seen that a good linear relationship does exist between the two values of  $H$ : the slope of the straight line in Fig. 5 is close to unity. Table III collects the slopes and correlation coefficients for all the tested liquids on the same screen ruling (50 cm<sup>-1</sup>); a good agreement between the calculations and the experiments may be observed. The significance of this result is that the approach of Cassie and Baxter is valid in the case of advancing and receding contact angles, and not only for the equilibrium contact angle of Young's equation.

### Conclusion

Our experiments were conducted on classical offset plates that are widely used in the graphic arts industry. They aimed to examine if it was possible to predict the behavior of a fountain solution when it is deposited on a screened area, by the use of two classical screen rulings. The tested tool for such predictions was the contact angle, which is the best way to describe the wetting phenomena occurring on this kind of surface.

Two distinct approaches were tested and both of them globally turned out to be in agreement with the experiments. On the one hand, Shanahan and Di Meglio consider a mechanism ("shadowing effect") to explain the hysteresis phenomenon itself; these authors derive rather complicated formulae. Mainly due to a relatively large uncertainty on low contact angle measurements on alumina (chosen as the reference substrate), it was not uneasy to derive reliable values of  $H_{cal}$  by their formulae, especially in the cases where the test liquids, water and glycerol, did not wet the reference surface. Nevertheless, the situation was slightly more comfort-

TABLE III. Slopes of Linear Correlations

| Liquid         | Slope | Correlation coefficient |
|----------------|-------|-------------------------|
| Water          | 0.95  | 0.96                    |
| Glycerol       | 0.98  | 0.97                    |
| Fount. sol. 2% | 1.03  | 0.99                    |
| Fount. sol. 3% | 0.86  | 0.98                    |
| Fount. sol. 5% | 1.03  | 0.99                    |

able with the tested fountain solutions, due to a complete wetting of the non-image areas of the plate. Thus, we think that shadowing effect at least qualitatively governs what happens on the screened areas of any offset plate. Moreover, it is likely that the analysis of Shanahan and Di Meglio could be effective for studying the new generation of offset plates which are processed by laser beams in "Computer-To-Plate" systems.

On the other hand, Cassie and Baxter have proposed a semi-empirical linear relation for the evaluation of the average contact angle on a heterogeneous surface. Their formula only requires the knowledge of contact angles on the two kinds of surfaces that are present in a screened area (provided their relative areas be given). Our results show that their model may be extended for quantitative evaluations of advancing and receding contact angles, but it does not give any valuable information about the physical phenomena themselves.

Some features remain to be elucidated, such as:

- the effect of the screen ruling, by the use of other values of this parameter in order to extend their variation range;
- the unexpected validity of the shadowing effect when the relative surface of the so-called "defects" becomes equal to or larger than that of the "reference".

Finally, it is useful to add that it would be interesting to also take surface roughness into account, because as is well known<sup>4</sup>, it is an important cause of contact angle variations. One conjectural reason for this is the similarity between the dimensions of main asperities and the thicknesses of ink and fountain solution films on classical offset surfaces: both are found in the range of a few micrometers. ▲

### References

1. J. MacPhee *Fundamentals of lithographic printing, 1: Mechanics of printing*, GATF Press, Pittsburgh, 1998.
2. D. H. Kaelble, P. J. Dynes and D. Pav, Surface energetics analysis of lithography, *Adhesion Sci. Tech.* **9B**, 735 (1975).
3. P. Aurenty, S. Lemery and A. Gandini, Dynamic spreading of fountain solution onto lithographic anodized aluminium oxide, *TAGA Proc.*, 563 (1997).
4. R. N. Wenzel, *Ind. Eng. Chem.* **28**, 988 (1936); cited in Refs. 3, 5 and 7.
5. A. B. D. Cassie and S. Baxter, Wettability of porous surfaces, *Trans. Faraday Soc.* **40**, 546, (1944).
6. A. B. D. Cassie, Contact angles, *Disc. Faraday Soc.* **3**, 11 (1948).
7. J. F. Joanny and P. G. de Gennes, A model for contact angle hysteresis, *J. Chem. Phys.* **81**, 552 (1984).
8. M. E. R. Shanahan, On the form of a locally perturbed liquid/solid/fluid triple line, *J. Phys. D (Appl. Phys.)* **23**, 703 (1990).
9. J. M. Di Meglio, Contact angle hysteresis and interacting surface defects, *Europhys. Lett.* **17**, 607 (1992).
10. J. M. Di Meglio and M. E. R. Shanahan, Effets coopératifs de défauts sur l'angle de contact: le phénomène d'ombrage, *C. R. Acad. Sci.* **316** (II), 1543 (1993).
11. M. E. R. Shanahan and J. M. Di Meglio, Wetting hysteresis: effects due to shadowing, *J. Adhesion Sci. Technol.* **8**, 1371 (1994).
12. A. Viallet, E. Rousset and G. Baudin, A simple apparatus for contact angle measurements by the heavy drop method, *Rev. Scient. Instr.* **70**, 4324 (1999).